Synthesis of Blend Polymer (PVA / PANI)/Copper (1) Oxide Nanocomposite: Thermal Analysis and UV-Vis Spectra Specifications

Raghad Subhi Abbas Al-Khafaji

Department of Physics, College of Education for Pure Science (Ibn - Al Haitham), University of Baghdad, Iraq

Abstract

   Copper (1) oxide nanoparticles together with matrix polymers of polyvinyl alcohol (PVA) and polyaniline (PANI) composite films were synthesized, as these materials are of importance in optoelectronic applications. Nanoparticles of Cu_2O were produced by chemical precipitation. Polymerization of aniline was carried out through polymerization in an acidic medium. Structural, thermal, and optical properties of $PVA+PANI/Cu_2O$ nanocomposite were inspected by x-ray diffraction (XRD), scanning electron microscopy (SEM), fourier-transform infrared (FTIR), differential scanning calorimeter (DSC) and ultraviolet-visible spectroscopy (UV-Vis spectroscopy). X-ray diffraction peaks at 29.53°, 36.34°, and 42.22° indicated the presence of cuprous oxide nanoparticles, having high dispersions and limited size distributions. The estimated average size of Cu_2O nanoparticles was ~ 17.1525 nm. A characteristic peak at around $2\theta = 18.5°$ was attributed to periodical parallel and perpendicular polymer chains, which denoted the formation of PANI. SEM results indicated the symmetrical dispersion of Cu_2O nanoparticles inside the hybrid polymer of PVA and PANI matrix, being potentially useful for encapsulation and acting as a good capping agent. FTIR results established the formation of PANI and Cu_2O with nanocrystalline nature. DSC results revealed the appearance of one single peak of T_g which decreased with Cu_2O content of 4% wt, followed by an increase of that value by increasing Cu_2O content up to 16%wt. Thermogram analysis of the PANI and PVA embedded with Cu_2O form showed an exothermic peak at (240-292)℃ affiliated to the cross-linking reaction, while the T_m value of prepared nanocomposites is just about close to that of PVA polymer. The results indicated that there is an increase in thermal stability due to the presence of Cu_2O NPS within the matrix of polymers. The distinguishing peaks at 330, 347, and 457 nm which refer to PANI are assigned to $\pi-\pi*$ electron transitions among the benzenoid rings. The high absorption intensity of the peak at 470 nm for the blended PVA+PANI having 12% wt of Cu_2O NPS is assigned due to the inter-band transitions for electrons of the core copper as well as copper oxide. This points out that the increasing quantity of Cu_2O NPs leads to increases in the amounts of highly oxidized structures in PANI and decreases in the doping electrons and length of conjugation throughout the incorporation of Cu_2O NPs into PANI matrix. Depending on the practical results, it can be said that these polymeric nanocomposites can be efficiently used in photovoltaic technology applications.

Keywords: Polyaniline, cuprous oxide, nanocomposite, SEM, FTIR, thermal analysis, optical.

_____

*Email:raghadsubhiabbas@yahoo.com

تحضير متراكبات نانوية من خلائط بوليمر (PVA/PANI)/ اكسيد النحاس (I) : التحليل الحراري وخصائص طيف UV-Vis

رغد صبحي عباس الخفاجي

قسم الفيزياء، كلية التربية للعلوم الصرفة –ابن الهيثم، جامعة بغداد، بغداد، العراق.

الخلاصة

تم تحضيرأغشية متراكبات من جزيئات أكسيد النحاس النانوية (I) مع بوليمرات PVA و PANI. تم إنتاج الجسيمات النانوية Cu_2O عن طريق الترسيب الكيميائي ، لما لهذه المواد من اهمية في تطبيقات الالكتروبصريات. إجريت بلمرة الأنيلين من خلال طريقة البلمرة في وسط حمضي. فحصت الخصائص التركيبية والحرارية والبصرية للمتراكبات النانوية Cu_2O / PANI + PVA من خلال التحليلات XRD و FTIR و SEM و DSC و UV–VIS. تشير قمم حيود الأشعة السينية عند 29.53 درجة و 36.34 درجة و 42.22 درجة إلى وجود نحاسي النانوي، مع تشتت عالي وتوزيعات محدودة الحجم. متوسط الحجم المقدر لجسيمات النحاس النانوية في حدود17.1525 نانومتر. ذروة مميزة عند حوالي 18.5 = 2θ درجة تُعزى إلى التوازي الدوري والعمودي لسلاسل البوليمر التي تشير إلى تكوين PANI. يشير SEM إلى التشتت المتماثل للجسيمات النانوية Cu_2O داخل مصفوفة البوليمر الهجين PVA و PANI ،. يؤكد FTIR تكوين PANI و Cu_2O مع طبيعة بلورية نانوية. يظهر DSC واحدًا من ذروة T_g التي تتناقص مع محتوى 4 Cu_2O % بالوزن. تم الكشف عن زيادة في القيمة عن طريق زيادة محتوى Cu_2O حتى 16٪ بالوزن. يُظهر الرسم الحراري لـ PANI و PVA المضمن في شكل Cu_2O ذروة طاردة للحرارة عند (292–240) مرتبطة بتفاعل الارتباط المتقاطع ، T_m قريبة تقريبًا من قيمة PVA. تم تعيين القمم المميزة عند 330 و 347 و 457 نانومتر والتي تشير إلى PANI إلى – * الانتقال. تم تعيين كثافة امتصاص عالية تبلغ الذروة عند 470 نانومتر لـ PVA + PANI التي تحتوي على 12 ٪ وزن من Cu_2O NPS بسبب التحولات بين النطاقات لإلكترونات نواة النحاس وكذلك أكسيد النحاس.

1. Introduction

Cuprous oxide is a natural p-type semiconductor that is not - noxious and highly plentiful in the crust of the earth. It has a great coefficient of absorption which extends from the violet to green solar spectra, which enables it to convert solar energy to electrical or chemical energy. Cu_2O is considered as one of the most attractive inorganic systems with a wide range of applications in gas detecting, CO oxidation, photocatalysis, photochemical evolution of H_2 from water, and photocurrent generation [1-3]. Cu_2O nanoparticles can be produced by various processes, such as electrodeposition, chemical method, thermal relaxation, liquid - phase reduction, evaporation in vacuum, and green combination. Nanostructures with conducting polymers, like PANI and polypyrrole, along with their nano - dimensional composites, appeared as an attractive field of research that can lead to creating novel materials for recent technologies. The nano-dimensional condition of metal oxide/polymer composites reveals improved electrical and magnetic properties compared with primeval metal oxide and conduction polymers. In addition , these composites exhibit high stability in the air, chemistry, and electricity mediums, for example, transistors (field effect), as well as their ease of production [4,5]. The carriers of charge for the PANI are mostly regarded to be polarons and bipolarons, which are steadied by counter ions combined into the polymer during the preparation. Conductive polymers have lately become an area of widespread attention in the field of organic electronics due to their potential practical application in energy conversion designs such as photovoltaic and solar cells, biosensors, and others [6,7]. They also have a wide array of electrical properties which can make them easily well-ordered by changing their

states of oxidation and protonation [8-10]. However, the main difficulty related to the successful utilization of PANI is its poor mechanical solubility within aqueous and organic solvents. Enhancement of polyaniline properties can be accomplished either by developing composites and nanocomposites for aniline or blending them with polymers or inorganic materials which exhibit better mechanical and optical properties, along with the stability in the handling of PANI [11, 12]. Polyvinyl alcohol (PVA) insulating polymer is acknowledged as a water-soluble and crystalline vinyl polymer within hydroxyl (–OH) groups bonded to the carbon atoms in the backbone of a long – chain molecule. The technique of chemical reduction is commonly used for the production of Cu_2O NPs from Cu^{2+} salts. It includes reducing Cu^{2+} ions to Cu^+ with a reducing agent [13].

In this paper, a successful and environmentally safe pathway in preparing Cu_2O nanoparticles is described. This pathway was achieved by chemical precipitation of NPs surrounded by a matrix of PVA and PANI which prepared through polymerization, for the synthesis of nanocomposites at room temperature. The properties of PVA+ PANI /Cu_2O were examined by means of XRD, SEM, FTIR, DSC, and UV-Vis.

2. Methodology

Synthesis of inorganic nanoparticles is still a confronting task due to innate difficulties in the control of compositions and morphology. Cupric nitrate and sulfate salts and alkaline compounds (normally NaOH) are regularly utilized in the synthesis of Copper(I) oxide Cu_2O NPS. The procedure of chemical precipitations was adopted in the present study. Briefly, copper sulphate pentahydrate ($CuSO_4. 5H_2O$; 2.5g) was dissolved in deionized water (20ml). The solution was placed inside a round - bottom flask provided with a refluxing apparatus. The $CuSO_4. 5H_2O$ solution was preserved at a suitable temperature of about 100 ℃ with dynamic stirring. Then, an amount of 0.8g (0.5 molL^{-1}) solid NaOH (platelet) was dissolved in 50 ml deionized water and added to the 20 mL aqueous solution of $CuSO_4$ by continuous stirring. This resulted in the production of a large amount of blue $Cu(OH)_2$ precipitate which appeared instantly, where the temperature of crystallization was kept for 10 min. Then, 0.80g ascorbic acid dissolved in 40 mL of the deionized water was added drop by drop to the solution with strong stirring. Subsequently, the precipitates were heated up to 100 ℃ for additional 10 min. The solution was centrifuged at 6000 rpm for 30 minutes to separate the distilled water. Then, the product was rinsed with water, followed by ethanol, several times, and dried out in the air at room temperature. The colloidal dispersion of the brown-colored Cu_2O nanoparticles was prepared. The reaction temperature affects the size and shape of the producing cuprous oxide Cu_2O nanoparticles.

Polyaniline was prepared by following similar procedures used to oxidize 0.2 M aniline hydrochloride with 0.25 M ammonium peroxydisulfate within the aqueous middle [14]. Aniline hydrochloride purum (2.59 g, 20 mmol) was dissolved with distilled water in a volumetric flask to make a 50 mL solution. Ammonium peroxydisulfate (purum; 5.71 g, 25 mmol) was similarly dissolved in water to 50 mL. Both solutions were kept for 1 h at room temperature. Subsequently, they were mixed in a beaker, shortly stirred, and left to polymerize. After 24 h, the PANI precipitate accumulated on the filter was rinsed three times with 100 mL of 0.2 M hydrochloric acid, and similarly with acetone. Polyaniline (emeraldine) hydrochloride powder was dehydrated in the air and then in a vacuum at 60 °C. Extra polymerizations were performed in ice bath of about 0–2 °C. The acidity of the reaction mixture was raised by interchanging 10 mL of water with 10 mL of 10 M HCl in several times. PVA was dissolved utilizing distilled water in a beaker at the heating condition. Then, Cu2O NPs (0, 4, 8, 12, and 16 % wt) were added to about 15% wt of PVA and various percentages of PANI solution. Stirring was continued at a temperature of around 100 ℃ for 2 h. The resulting product was cooled at room temperature and dried in a hot air oven to obtain PVA + PANI/ Cu2O nanocomposite samples. Figure 1 clarifies the sequence of this

methodology. Thin films of a thickness range of 0.025-0.030 cm were tested using an X-ray diffractometer with radiation of Cu Kα (λ=1.5406 Å) (Shimadzu XRD – 6000). The XRD patterns were interpreted by matching the observed identical peaks with the standard pattern provided by JCPDS files. The surface morphology and particle size of the manufactured nanoparticles were examined by SEM (FEI Company, Inspect S50-Model). Moreover, FTIR spectrometer (Shimadzu IRAffinity-1S) was employed at a wavenumber range of 400-4000cm^{-1} to detect polymeric and some inorganic materials. The thermal transitions behavior of the prepared nanocomposite thin films was revealed by a differential scanning calorimeter (Shimadzu DSC-60) through a heating rate of 10°C/min. The optical UV- Vis spectra were verified in a range of 300 to 1100 nm using Shimadzu spectrophotometer UV-1800.
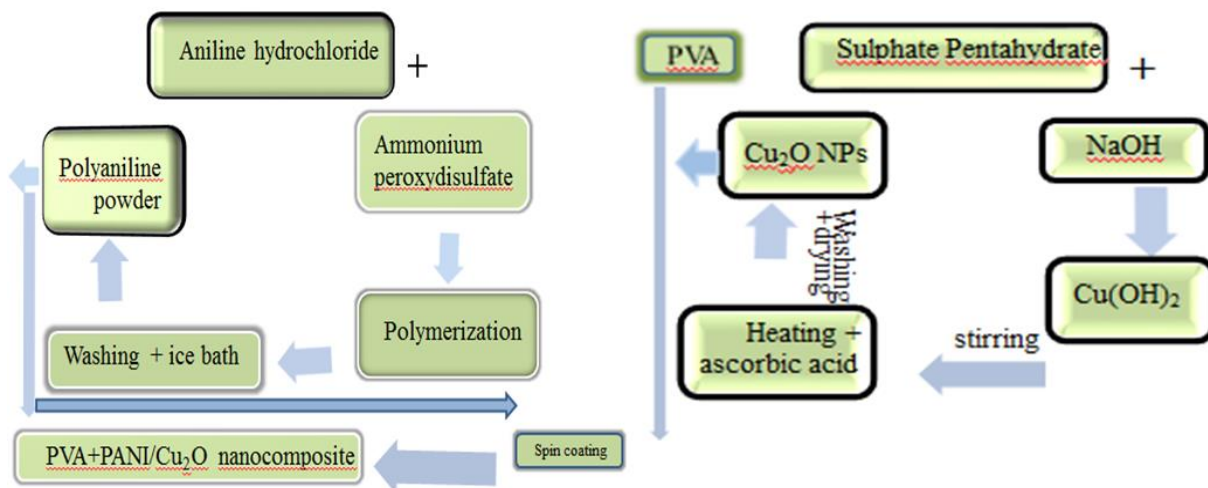

Figure 1- A flow chart showing the steps of nanocomposite preparation PANI+PVA/Cu$_2$O

3. Results and Discussion

X-ray diffraction assays infer a great deal of information about the crystal structure, crystallite orientation, and size of desired regions within materials. Figure 2 displays the X-ray diffraction patterns of PVA, PANI. their homopolymer blend, and their Cu$_2$O/(PANI + PVA) nanocomposites at RT and scan ranges of $10° \leq 2\theta \leq 80°$ and $5° \leq 2\theta \leq 80°$, respectively.

X-ray diffraction pattern of PVA 85%wt and PANI 15%wt blend (sample 5) is shown in Figure (2a). In this pattern, one main broad peak appeared around the diffraction angle of $2\theta = 19.72°$, corresponding to the (101) crystal plane of PVA. Also, the presence of the distinct crystal peak at $2\theta = 15.280°$, which is indicative of the semi - crystalline nature of PVA, was noticed. The crystallite nature of PVA results from the powerful intermolecular interactions between PVA chains through hydrogen bonds [13]. Besides, the XRD pattern reflects the characteristic peak around the diffraction angle $2\theta = 18.5°$, which can be attributed to the parallel and vertical cyclic polymer chains of PANI. The peak at about $2\theta = 20°$ is a confirmation of the distance between individual benzene rings within adjacent chains.

The peak centered around $2\theta = 25°$ can be appointed to the scattering of the PANI chains at inter-level spacing. The peak at $2\theta = 13.90°$ infers that the PANI polymer also has a certain degree of crystallinity (partial crystallization) [15, 16]. It is also clear from Figure (2a) that the XRD pattern of the PVA/PANI blend samples revealed the features of pure PVA, but with a lower intensity of the crystal peaks. The semi-crystalline structure is reduced upon mixing PVA with PANI in various concentrations. Moreover, some of the crystal peaks ($2\theta = 15.280°$, 25,654°, and 23.520°) are no longer noticeable because they are of low intensity in the XRD pattern of the blend polymers due to weak reflections from the arrangement of the

structure. For the semicrystalline-amorphous mixtures, the amorphous component may strongly adjust the crystallization behavior of the components. The miscibility of the amorphous components of the two homopolymers is likely. Thus, it can be suggested that the crystalline formulas in PVA do not prevent mixing between amorphous regions of polymers (conventional semi-crystalline) in blend systems [2,17].

The X-ray diffraction patterns of Cu_2O/(PANI + PVA) nanocomposites prepared with 16% wt% were studied in Figure (2b). This figure exhibits five discernible peaks that are perfectly indexed to crystalline Cu_2O NPS by standard JCPDS data (File No. 05-0667). The peaks at diffraction angles of 29.53°, 36.34°, 42.22°, 61.30°, and 73.47° were mapped to the corresponding crystal plans (110), (111), (200), (220), and (311) of the Cu_2O NPS nanoparticles. These nanoparticles revealed good crystallinity due to having sharp peaks in the XRD pattern and broadening peaks indicating that the crystallite size is small. The crystallite size of the prepared Cu_2O nanoparticles was calculated using Scherrer's equation [18].

Crystallite size calculation by XRD is a generally accepted quantitative method in the scientific community. The average size of copper oxide nanoparticles is estimated to be around 17.1525 nm. In the XRD pattern, the locations of the peaks are in good agreement with references (JCPDS 05-0667). The XRD pattern of the PVA+PANI/Cu_2O composite determines the diffraction of Cu_2O nanoparticles, including discrete peaks which can be exquisitely indexed towards crystalline Cu_2O nanoparticles. From the XRD patterns of the blend and nanocomposites, it was demonstrated that Cu_2O remains stable in structure even though it is dispersed in PVA + PANI during the polymerization reaction. Figure (2b) shows the presence of the PANI + PVA and Cu_2O NPS copolymers due to the appearance of peaks obtained from these materials in the nanocomposites. However, the Cu_2O NPS peak is
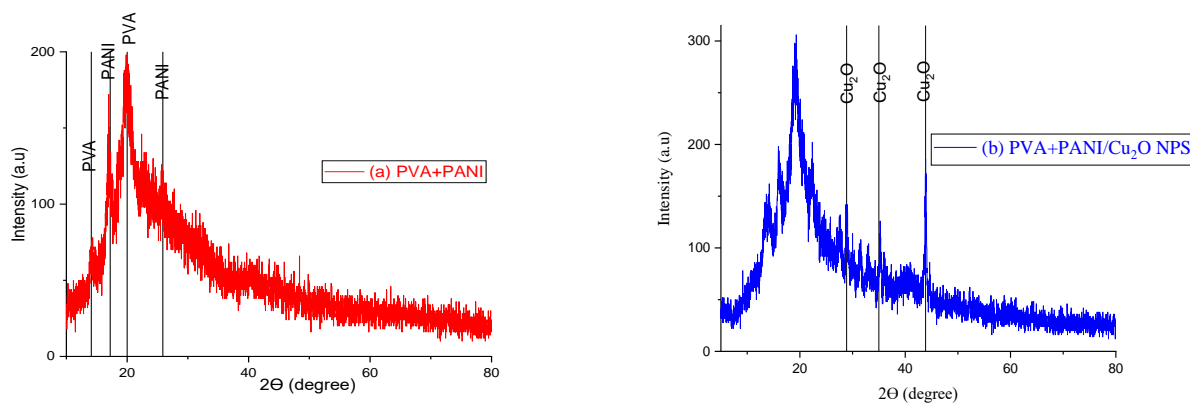

Figure 2- XRD analysis spectrum for (a)) blend of 15% wt PANI and 85% wt PVA(sample 5), and (b) PVA+ PANI/Cu_2O nanocomposites at 16 % wt.

broadening, with a decrease in the intensity of the peaks for PANI and PVA. This shows the effect of Cu_2O NPS in the PANI and PVA matrix. Moreover, in the prepared nanocomposites samples, the Cu_2O intensity peak (not visible in the diffraction) was hidden by the presence of the PVA + PANI mixture, indicating the complete precipitation of PANI and PVA within the Cu_2O NPS [19-21].

The blend of PVA + PANI and its PVA + PANI/Cu_2O nanocomposites were morphologically examined by SEM to estimate the average particles size as well as to verify the information about the surface texture and the presence of formed Cu2O nanoparticles.

Figure 3 shows different SEM magnified micrographs of sample 4 nanocomposites with 16% Cu_2O concentration and sample 5 without the addition of Cu_2O.

The images in Figure 3a and b show 5 separate polyaniline nanoparticles that are uniformly assembled. The particles are rod-shaped, referring to a polyaniline particle of irregular morphology and high heterogeneity within the chain dimensions. The microcrystalline nature of PANI is due to partial agglomeration in the lattice structure. The images in Figure 3a/4 show well-separated, regular, spherical fly ash-shaped Cu2O NPS with an estimated average diameter ranging from 163 to 381 nm, indicating the occurrence of agglomeration. Figure (3a/4) shows Cu_2O NPS as a good and homogeneous filler that is slowly incorporated into the composite matrix of PVA + PANI due to the strong chemical attraction of Cu and polyaniline nitrogen. Thus, the PVA + PANI polymer blend is an excellent host matrix to avoid the accumulation of copper nanoparticles and is useful for encapsulation, acting as a good covering agent and providing chemical and environmental stability [22, 23].
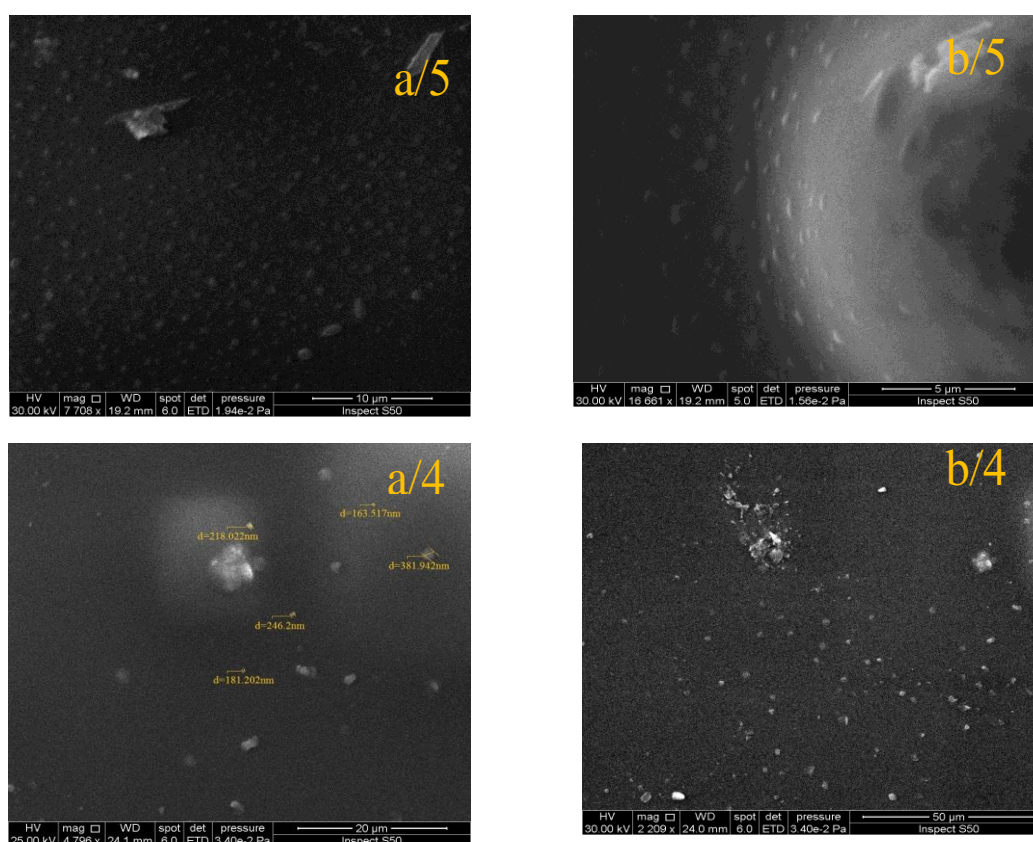

Figure 3- Scanning micrograph at different magnifications. Symbols a/5 and b/5 referring to sample 5 (blend of 15% wt PANI and 85% wt PVA), and a/4 and b/4 for sample 4 (PVA+ PANI/Cu_2O 16 % wt of nanocomposites).

Fourier transform infrared spectroscopy in the wave range of 400-4000 cm was applied to provide auxiliary data on the properties of each element included in the composite mixture of polyvinyl alcohol and polyaniline, along with its Cu_2O- reinforced nanocomposites, as shown in Figure 4. Figure (4a) manifests FTIR spectra of synthesized PANI blended with PVA. The characteristic peaks of PANI include broad peaks that range 3016.67 - 3455 cm^{-1} corresponding to N–H stretching vibrations of secondary amine, a sharp peak at 1540 cm^{-1} (C=C stretching of the quinoid ring (N=Q=N)), 1470 cm^{-1} ((C=C stretching vibration of the benzenoid ring (N-B-N)), 1240 (C - N stretching of secondary aromatic ring), 1100 cm^{-1} (Aromatic C–H in-plane bending vibrations), and 804.32 cm^{-1} (Aromatic C–H out-of-plane bending vibrations). These peaks match well with those mentioned in previous works [24,

25]. Figure (4a) illustrates characteristic bands of bending and stretching vibrations of O–H, C–H, and C–O groups, ascribed to polyvinyl alcohol. The peak at 3374 cm^{-1} is the specific band of the O–H stretching vibrations for PVA. The bands detected at 1580-1650 cm^{-1} are appointed to the stretching mode for C=O and C=C groups in chains of the polymer. Two strong peaks at 1418 and 1340 cm^{-1} are recognized to CH2 and vibrations of (CH + OH) groups. Furthermore, the band at peak 1120 cm^{-1} is appointed to the C–O stretching mode [26, 27]. The FTIR spectra of the prepared nanocomposites are shown in Figure (4b). Cu_2O displays an absorption peak at about 622 cm−1, which determines the Cu(I)-O vibration signal that is well-matched with that of Cu_2O reported in previous works [21]. This indicates the formation of Cu_2O particles in the matrix network.
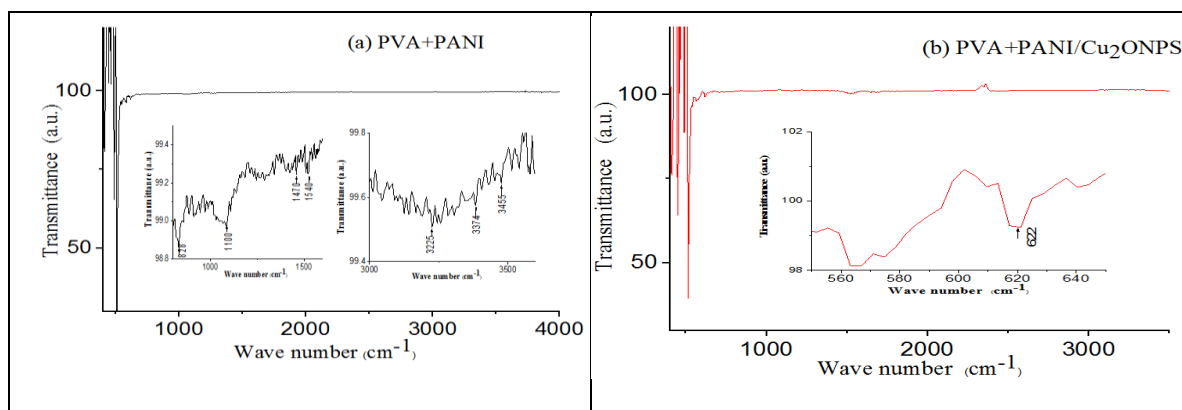

Figure 4-. Fourier transform infrared spectroscopy with wave numbers for (a) blend PVA+PANI related to sample 5; the inset figures illustrate absorption peaks in ranges of 500-1500 cm^{-1} and 3000-3500 cm^{-1}, (b) blended cuprous oxide at 16 %wt of nanocomposites related to sample 4; the figure illustrate absorption peaks in range of 540-640 cm^{-1}.

DSC technology provides data for glass transition (T_g), melting point (T_m), crystallization temperatures (T_c), as well as specific capacitance (C_p) for each process. Figures 5 and 6 show the heat flux and specific heat curves in the temperature range from 15 °C upward to 300 °C for samples prepared with and without copper oxide nanoparticles, respectively.

The values of the transition temperature, specific heat, and fusion heat associated with each transition, obtained by DSC analysis curves for the blend and doped samples, are listed in Table 1. Sample 5 of the PVA + PANI blend shows two endothermic peaks. The first peak at 44.30 °C is assigned as a thermal effect due to moisture evaporation (water removal), the presence of impurities from the polymer blend sample, and glass transition. The second peak indicates a sharp transition due to an endothermic melting at 210.2 °C with an enthalpy of 0.431J/g. However, the acquired value of T_m (210.2 °C) is in agreement with that found by Sakelariou *et al*. [28].
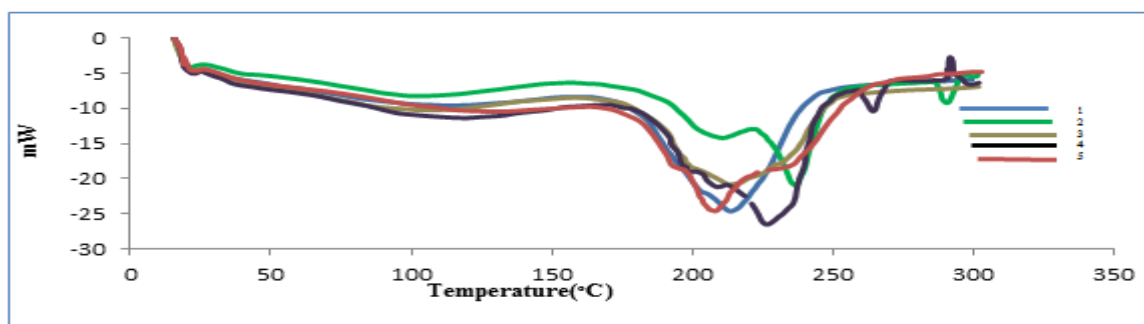

Figure 5- Heat flow at a range of temperature from 15°C up to 300°C for different concentrations of nanocomposites.

It is fascinating to show how the heat transfer of PVA + PANI varies after adding varying concentrations of Cu_2O nanoparticles. It is observed that the DSC thermograms for all samples prepared from PVA+PANI and PVA+PANI/Cu_2O show one glass transition (T_g) peak, which decreases with the increase in Cu_2O 4% wt concentration. Then, an increase in the value of T_g is observed by increasing the Cu_2O concentration up to 16 %wt for the prepared nanocomposite samples. We note that the obtained T_g values indicate the miscibility of the mixing system. The broadening of the peaks depends on the decrease in the OH content. The PVA hydroxyl groups are largely crosslinked by hydrogen bonding, resulting in maximum temperatures of glass transition (T_g), as in sample 2.

The thermal graph of the blend of polyaniline and polyvinyl alcohol shows an exothermic peak at 240-280 ℃ that may be related to cross-linking reactions [29-31]. Another exothermic peak can be set at 292℃ which refers to sample 4 with a concentration of 16%wt of copper oxide nanoparticles, due to the cross-linking/oxidation in the backbone compound. The cross-linking in these polymers is irreversible and thus will only be detected when the polymer is first heated. Thus, based on the thermal profile of these materials, we can state that, among polyvinyl alcohol, polyaniline, and the composites of Cu_2O nanoparticles, cross-linked or oxidative reactions start at a higher temperature than that of the composites, which indicates the stability of the PANI blend composites. The data in Table 1 point out that the melting points (T_m) for the nanocomposite samples are closely around those for the PVA and PANI polymers , indicating the miscibility of the blend system. Also, it seems that the variations in shape and area were due to the diverse degrees of crystallinity found in the samples with different concentrations of Cu2O nanoparticles. The decrease in the heat of fusion and the increase in Tm propose that the crystallinity and faultlessness structure of the crystals are decreased with increasing the degree of cross-linking. This could change the crystalline structure, which might affect polymer-polymer interaction in the amorphous phase; therefore, trouble in the crystals is created, decreasing the enthalpy (heat of fusion) for phase transitions. DSC plot of the nanocomposites showed the presence of a common sharp peak at 230.3℃. This confirms the existence of a monoclinic phase dependent on the copper ion for the oxidation state, which is attributed to Cu_2O [32-34].
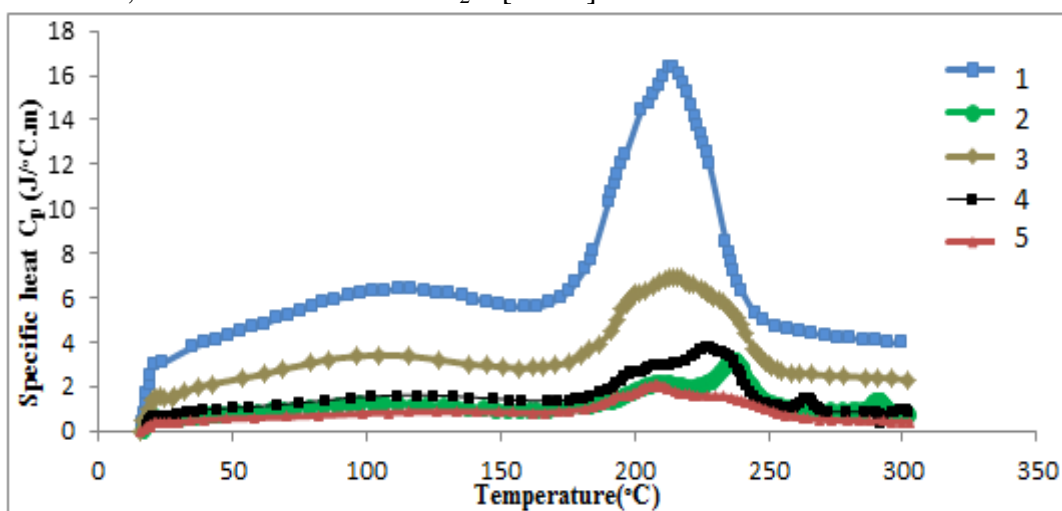

Figure 6- Specific heat with temperature at range from 15°C up to 300°C for different concentrations of Cu_2O nanocomposites.

Table 1- Summarized values for DSC investigation of T_g, T_m, C_p, and heat of fusion for each concentration of nanocomposites.

Sample No	Con % wt PANI	Con % wt PVA	Con % wt Cu_2O	T_g (℃)	T_m (℃)	C_p at T_m (J/℃.m)	Heat of fusion (ΔH, J/g)
1	15	81	4	42.68	217.61	14.560	3.170
2		77	8	46.20	238.74	2.984	0.708
3		73	12	45.76	218.10	7.149	1.560
4		69	16	45.74	230.30	3.525	0.823
5		85	-	44.30	210.20	1.966	0.431

Optical spectroscopy is a significant technique for finding out the conduction states that correspond to the absorption bands of conductive polymers.

Figure 7 shows the optical absorption as a function of the wavelength (λ) of the prepared PVA + PANI blend samples and their PVA + PANI/Cu_2O nanocomposites at different weight ratios of Cu_2O NPS.

We observe distinct peaks at 330, 347, and 457 nm, indicating the - * transition of PANI which is attributed to the benzenoid ring related to the extent of coupling between adjacent phenylene rings in the polymeric chains and the system caused by the accumulation. This leads to increased coupling and thus reduced bandgap.

The * benzenoid ring transition and polaron band formation are responsible for the increased electric conductance of the nanocomposites. The intense band decrease at about 300 nm might be due to the n − * transition. The peaks at 400, 420, and 435 nm could be attributed to the polaron - * transition as well as the electron transition from the benzenoid ring to the quinonoid ring [10].

The absorption peaks of the low concentration (4% wt) Cu_2O NPS nanocomposite in figure- (7a) show a blue shift towards PANI with weak adsorption intensity for Cu_2O. This indicates the formation of the Cu_2O/PANI nanocomposite due to the incorporation of the Cu_2O content into the PANI matrix.

In figure- (7c), which is dedicated for nanocomposite sample 3 of PVA + PANI blended with 12 wt% Cu_2O NPS, we observe a high peak of absorption intensity due to electrons between the inter-band transitions of Cu core and Cu oxide.

Increasing the amount of Cu_2O NPS content leads to the severe change of the characteristic peaks of PANI and the absorption peaks of Cu_2O NPS in the nanocomposites. This indicates that the increasing amount of Cu_2O NPS increases the amount of highly oxidized structures in PANI [8-10].

Figure -7 shows the absorption peaks of high intensity with the blue shift of polyaniline from the positions of the regular peaks, indicating that the addition of Cu_2O nanoparticles as a filler in the polyaniline and polyvinyl alcohol matrix affects the absorption spectra of the prepared nanocomposites.

The less intense absorption peaks are due to Cu_2O within the nanocomposite, which indicates the interactions between Cu_2O within the polyaniline and thus shows the polaron construction as well as the charges bipolaron carrier in the nanocomposite [13-15].
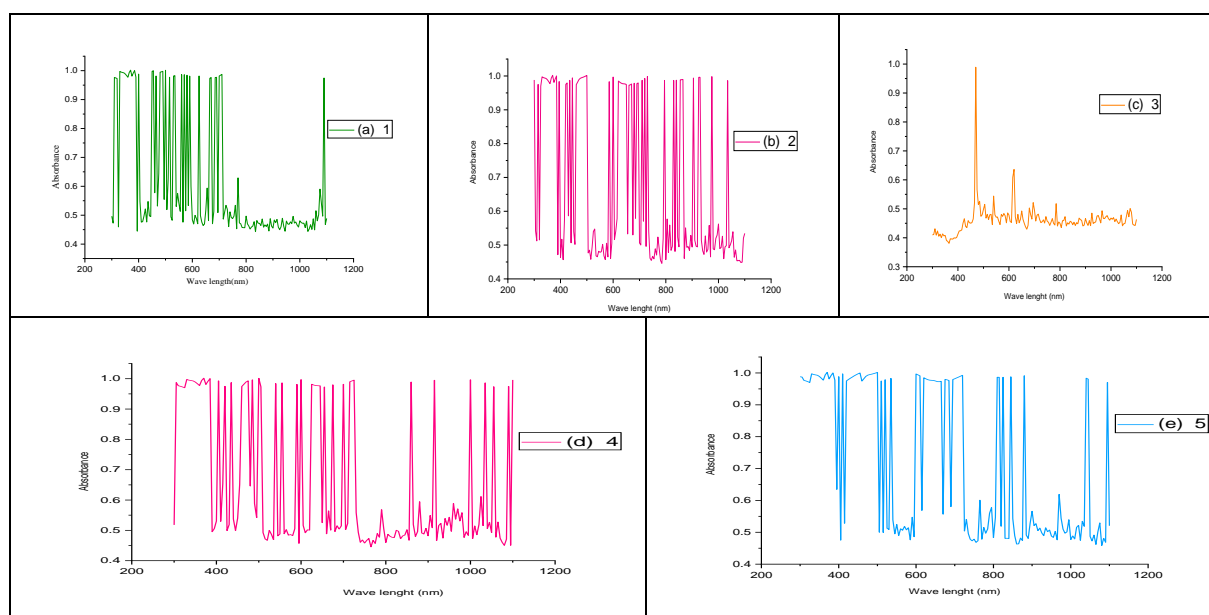
Figure 7- Optical absorbance in wavelength (λ) for (a-d) PVA+PANI/ Cu$_2$O nanocomposites with 4, 8, 12, 16 wt.% Cu$_2$O NPS, respectively. (e): PVA+PANI prepared blended sample.

As stated previously by several researchers, doped composites of PANI polymer regularly display three characteristic absorption bands at ranges of 320−360, 400−450, and 740−950 nm [2, 35]. Firstly, the absorbance band develops from π−π*, indicating the electron transitions within the benzenoid section. Secondly and third absorbance bands are connected to the doping levels and the construction of polarons (segments of quinoid), one by one. For the absorption spectra of PANI +PVA/Cu$_2$O samples, a shoulder is centered at around 300nm, and a broadening band is centered at 450 nm.

In the visible absorption range, the PVA + PANI/Cu$_2$O nanocomposites also have a strong absorption at the wavelength of 591 nm. It should be noted that, in the visible spectra, the morphology, size, and crystallinity of the prepared nanoparticles affect the locations of the resulting optical absorption peaks.

Since PVA is a preferred hydrophilic and environmentally-safe polymer, it was selected as a stabilization and dispersion matrix to build a stable Cu$_2$O polymer composite structure.

It is shown that the introduction of Cu$_2$O nanoparticles affects the doping of conductive polyaniline. This effect leads to the interfacial reaction of polyaniline and Cu$_2$O NPS. The extinction coefficient designates the properties of a material exposed to light of a given wavelength. It also indicates the absorption variations when an electromagnetic wave propagates through the material. Figure - 8 exhibits the extinction coefficient (k) values (k = αλ / 4π), correlated with the absorption coefficient. It can be seen that a high peak of extinction coefficient (k) (0.00047) is reached at 470 nm in the prepared sample 3, with 12% wt of Cu$_2$O NPS, which possesses a high adsorption coefficient as explained above.
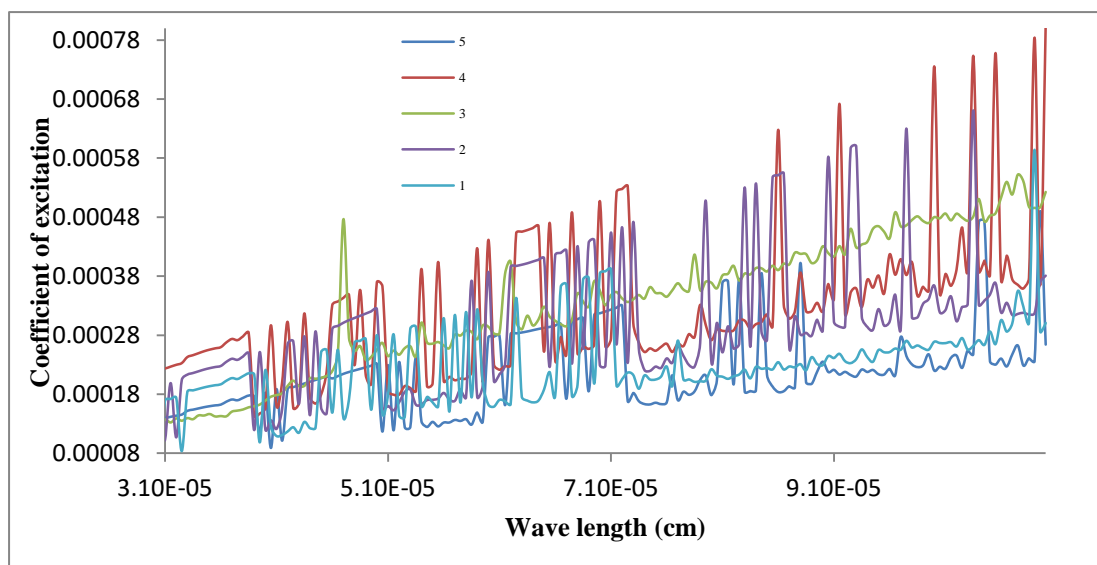
Figure 8- Optical spectra related to extinction coefficient of nanocomposites with variation concentrations of Cu_2O NPS.

5. Conclusions

A novel, simple, and time- and cost-effective method was developed for preparing thick films of polyvinyl alcohol and polyaniline composites supported by cuprous oxide nanoparticles.

Cu_2O nanoparticles were prepared by chemical precipitation and chemical polymerization methods. Aniline was polymerized in the acidic medium at RT. The structural, thermal, and optical properties of the PVA + PANI/Cu_2O nanocomposites were investigated by XRD, SEM, FTIR, DSC and UV-Vis spectra. The results showed that the prepared Cu_2O nanoparticles have a highly uniform dispersion and limited size distributions within the nanoscale. The differential scanning calorimeter analysis displayed a single glass transition peak. The melting point values of the nanocomposite samples are very close to those of PVA. Thermal investigation indicated that there is an increase in thermal stability due to the presence of Cu_2O NPS within the matrix of polymers, compared to that of pure polymers ,i.e thermal degradation happen at higher temperatures.

The high absorption intensity peak at 470 nm appeared in the nanocomposite sample 3 due to the inter-band transitions of the Cu core electrons and Cu oxide. This indicates that increasing the amount of Cu_2O NPS leads to an increase in the quantity of the highly-oxidized structures in PANI and a decrease in the doping electrons and coupling length during the incorporation of Cu_2O NPS into the PANI matrix.

Acknowledgements

References

[1]   Jha, V. K. " Synthesis Of Nanosized Copper Oxide Particles Using Hydrothermal Treatment", *Nep. J. Integrated Sciences*. vol. 2, pp. 42, 2012.

[2]   Jundale, D., Navale, S., Khuspe, G., Dalavi, D., Patil, P. and Patil, V. "Polyaniline–CuO hybrid nanocomposites: synthesis, structural, morphological, optical and electrical transport studies", *Journal of Materials Science: Materials in Electronics*. vol. 24, pp. 3526, 2013. https://doi.org / 10. 1007/s10854-013-1280-

[3] Neha, T., Surendra K., Taimur A. " Wet Synthesis of Copper Oxide Nanopowder", *International Journal of Green Nanotechnology: Materials Science & Engineering*. vol. 1, pp. M67–M73, 2009.

[4] Khan, M. M. R., Wee, Y. K. and Mahmood, W. A. K. "Effects of CuO on the morphology and conducting properties of PANI nanofibers". *Synthetic metals*. vol. 162. Pp. 1065, 2012. https://doi.org/10.1016/j.synthmet.2012.05.009

[5] Korzhavyi, P. A. and Johansson, B. "Literature review on the properties of cuprous oxide Cu 2 O and the process of copper oxidation", *Swedish Nuclear Fuel and Waste Management Co,* pp. 1-41, 2011.

[6] Linganathan, P., Sundararajan, J. and Samuel, J. M. "Synthesis, characterization, and photoconductivity studies on poly (2-chloroaniline) and poly (2-chloroaniline)/CuO nanocomposites", *Journal of Composites*. 2014.

[7] Liu, G., He, F., Li, X., Wang, S., Li, L., Zuo, G., Huang, Y. and Wan, Y. "Three-dimensional cuprous oxide microtube lattices with high catalytic activity templated by bacterial cellulose nanofibers", *Journal of Materials Chemistry*. vol. 21, pp. 10637, 2011. https://doi.org /10.1039 /C1JM11432H

[8] Madani, M. "Structure, optical, and thermal decomposition characters of LDPE graft copolymers synthesized by gamma irradiation", *Current Applied Physics*. vol. 11, pp. 70, 2011. https://doi.org/10.1016/j.cap.2010.06.021

[9] Mohamed Azharudeen, A., Karthiga, R., Rajarajan, M., and Suganthi, A. "Enhancement of electrochemical sensor for the determination of glucose based on mesoporous VO2/PVA nanocomposites", *Surfaces, and Interfaces*. vol. 16, pp. 164, 2019. https://doi.org/ 10.1016 /j. surfin .2019.05.005

[10] Mugwang'a, F., Karimi, P., Njoroge, W., Omayio, O., and Waita, S. "Optical characterization of Copper Oxide thin films prepared by reactive dc magnetron sputtering for solar cell applications" 2012. https://doi.org/10.1515/9783486751222-002

[11] Murali, D. S., Kumar, S., Choudhary, R., Wadikar, A. D., Jain, M. K. and Subrahmanyam, A. "Synthesis of Cu_2O from CuO thin films, Optical and electrical properties", *AIP Advances*. vol. 5, pp. 047143, 2015.

[12] Nasir, A., Masood, F., Yasin, T. and Hameed, A. "Progress in polymeric nanocomposite membranes for wastewater treatment: Preparation, properties and applications", *Journal of Industrial and Engineering Chemistry*. vol. 79, pp. 29, 2019. https://doi.org/10.1016 /j.jiec. 2019.06.052.

[13] Ramesh, C., Hariprasad, M., Ragunathan, V. and Jayakumar, N. "A novel route for synthesis and characterization of green Cu_2O/PVA nanocomposites", *European Journal of Applied Engineering and Scientific Research*. vol. 1, pp. 201, 2012.

[14] Stejskal, J. and Gilbert, R. "Polyaniline. Preparation of a conducting polymer" (IUPAC technical report), *Pure and Applied Chemistry*. vol. 74, pp. 857, 2002. https://doi.org/10.1351 /pac 200 274050857

[15] Nayak, S. "Study on the optoelectronic properties of UV luminescent polymer: ZnO nanoparticles dispersed PANI", *Journal of Materials*. vol. 2013, pp. 1, 2013. https://doi.org/10.1155 /2013 /473217

[16] Ohji, T., Jeong, Y. K., Choa, Y. H. and Niihara, K. "Strengthening and toughening mechanisms of ceramic nanocomposites", *Journal of the American Ceramic Society*. vol. 81, pp. 1453, 1998. https://doi.org/10.1111/j.1151-2916.1998.tb02503.x

[17] Aslam, M., Kalyar, M. A. and Raza, Z. A. "Fabrication of nano-CuO-loaded PVA composite films with enhanced optomechanical properties", *Polymer Bulletin*, 2020. https://doi.org/10. 1007 /s00289-020-03173-9

[18] Harold P. Klug and Leroy E. Alexander. "*X-ray diffraction procedures for polycrystalline and amorphous materials". Wiley, New York*, 1954. . https://doi.org/https: //doi.org/10. 1002/pol .1955.120178412

[19] Saeednia, S., Iranmanesh, P., HATEFI, A. M. and Sinaei, S. "Synthesis of Cuprous Oxide by Thermal Treatment in Liquid Paraffin" vol. 1, 2015. https://doi.org/10.7508/JNS.2015.03.012

[20] Senthilkumar, T. and Kumar, S. "Evaluation of Hardness Test of Silicon Carbide Particulated Aluminium Metal Matrix Composites", *Int. J. Res. Comput. Appl. Rob*. vol. 3, pp. 74, 2015. https://doi.org/10.18831/came/2016021002

[21] Sathish Mohan, B., Ramadevi, D. and Keloth, B. "A Facile Synthesis of Cu2O and CuO Nanoparticles Via Sonochemical Assisted Method", *Current Nanoscience*. vol. 15, pp. 209, 2019. http://dx.doi.org/10.2174/1573413714666180530085447

[22] Siva, M., Rajesh, R., Pugazhendhi, S. and Sivapragash, M. "Effect of Microstructure and Hardness Properties of Al2011 based Composites for Titanium Di Boride using Stir Casting Method", *International Journal of Mechanical and Production Engineering Research and Development (IJMPERD)*. vol. 7, pp. 187, 2017.

[23] Soytaş, S. H., Oğuz, O. and Menceloğlu, Y. Z. 9 - Polymer Nanocomposites With Decorated Metal Oxides. In K. Pielichowski & T. M. Majka (Eds.), *Polymer Composites with Functionalized Nanoparticles*: vol. 287, 2019. https://doi.org/10.1016/B978-0-12-814064-2.00009-3

[24] Sydulu Singu, B., Srinivasan, P. and Pabba, S. "Benzoyl Peroxide Oxidation Route to Nano Form Polyaniline Salt Containing Dual Dopants for Pseudocapacitor", *Journal of The Electrochemical Society*. vol. 159, pp. A6, 2011. https://doi.org/10.1149/2.036201jes

[25] Trchová, M., Jasenská, D., Bláha, M., Prokeš, J. and Stejskal, J. "Conducting polyaniline prepared in the solutions of formic acid: Does functionalization with carboxyl groups occur". *Spectrochimica Acta Part A: Molecular and Biomolecular Spectroscopy*. vol. 235, pp. 118300, 2020. https://doi.org/https://doi.org/10.1016/j.saa.2020.118300

[26] Shojaee Kang Sofla, M., Mortazavi, S. and Seyfi, J. "Preparation and characterization of polyvinyl alcohol/chitosan blends plasticized and compatibilized by glycerol/polyethylene glycol", *Carbohydrate Polymers*. vol. 232, pp. 115784, 2020. https://doi.org/https://doi.org/10.1016/j. carbpol. 2019.115784

[27] Hajipour, A. R. and Mohammadsaleh, F. "Polyvinyl alcohol-stabilized cuprous oxide particles: efficient and recyclable heterogeneous catalyst for azide-alkyne cycloaddition in water at room temperature", *Journal of the Iranian Chemical Society*. vol. 12, pp. 1339-, 2015. https://doi.org/10.1007/s13738-015-0599-7

[28] Sakellariou, P., Rowe, R. and White, E. "The thermomechanical properties and glass transition temperatures of some cellulose derivatives used in film coating", *International journal of pharmaceutics*. vol. 27, pp. 267, 1985. https://doi.org/10.1016/0378-5173(85)90075-4

[29] Subrahmanyama, A., Geethaa, V., Alakanandanac, A. and Kumard, J. S. "Mechanical and electrical conductivity studies of PANI-PVA and PANI-PEO blends", *International Journal of Material Science*. vol. 2, pp. 27, 2012.

[30] Suleiman, M., Mousa, M., Hussein, A., Hammouti, B., Hadda, T. B. and Warad, I. "Copper (II)-oxide nanostructures: synthesis, characterizations and their applications-review", *Journal of Materials and Environmental Science*. vol. 4, pp. 792, 2013.

[31] Tamayo, L., Azócar, M., Kogan, M., Riveros, A. and Páez, M. "Copper-polymer nanocomposites: An excellent and cost-effective biocide for use on antibacterial surfaces", *Materials Science and Engineering: C*. vol. 69, pp. 1391, 2016. https://doi.org/10.1016/j.msec.2016.08.041

[32] Topnani, N., Kushwaha, S. and Athar, T. "Wet synthesis of copper oxide nanopowder". *International Journal of Green Nanotechnology: Materials Science & Engineering*. vol. 1, pp. M67, 2010. https://doi.org/10.1080/19430840903430220

[33] Umoren, S. A. and Solomon, M. M. "Protective polymeric films for industrial substrates: A critical review on past and recent applications with conducting polymers and polymer composites/nanocomposites", *Progress in Materials Science*. vol. 104, pp. 380, 2019. https://doi.org/10.1016/j.pmatsci.2019.04.002

[34] Safa, K., Raied, K. "Studying the Effect of Annealing on Optical and Structure Properties of ZnO Nanostructure Prepared by Laser Induced Plasma". *Iraqi Journal of Science.* vol. 60, no. 10, pp. 2168, 2019.

[35] Yasir, Y., Ghazwan, G., Marwan, H. "Irradiation Effects on The Sensitivity of ZnO Thin Films Synthesized on Glass Substrate by Sol-gel Method", *Iraqi Journal of Science*. vol. 61, no. 1, pp. 130-137, 2021.